

Article

# Effects of Cholestasis Induced by ANIT on Liver Function and Important Signaling Pathways in Rats

Reham Hassan Thamer\*<sup>1</sup>

1. Department of Clinical Laboratory Sciences, Pharmacy College, Tikrit University, Tikrit, Iraq

\*Correspondence: [Reham\\_h\\_th@tu.edu.iq](mailto:Reham_h_th@tu.edu.iq)

**Citation:** Thamer R. H. Effects of Cholestasis Induced by ANIT on Liver Function and Important Signaling Pathways in Rats. American Journal of Biology and Natural Sciences 2026, 3(1), 41-53.

Received: 08<sup>th</sup> Dec 2025

Revised: 22<sup>nd</sup> Dec 2025

Accepted: 29<sup>th</sup> Dec 2025

Published: 06<sup>th</sup> Jan 2026



**Copyright:** © 2026 by the authors. Submitted for open access publication under the terms and conditions of the Creative Commons Attribution (CC BY) license (<https://creativecommons.org/licenses/by/4.0/>)

**Abstract:** This study was designed to study the effects of alpha-naphthyl isothiocyanate (ANIT) on vector liver function and histological changes in Wistar rats (focusing on biochemical markers and important signaling pathways related to cholestasis). Ten male rats were used and divided in two groups, a control group which received corn oil and an ANIT group that received ANIT orally at the dose of 100 mg/kg. Blood collection was performed after 48h to determine serum liver enzymes (ALT, AST, ALP, GGT), total bilirubin (TSB) and total bile acids (TBA). In addition, histopathological examination of liver sections stained with H&E was also performed for the evaluation of tissue injury. The results showed a significant increase in the levels of all parameters measured in ANIT group compared with the control. The results showed ALT level was increased from 26.80 ± 1.10 to 47.02 ± 1.64 I.U/L and AST level was increased from 27.56 ± 2.40 to 55.07 ± 2.81 I.U/L. ALP level was increased from 100.68 ± 2.02 to 353.45 ± 36.37 I.U/L and GGT level was increased from 236.82 ± 14.83. These findings provide clear evidence that ANIT induces acute cholestasis that is associated with extensive hepatic injury. The biochemical and the histological changes support the authenticity of ANIT as an experimental model of cholestasis. This data set provides a basis for studying FXR, Nrf2 and AMPK signaling pathways for the design of future therapeutic strategies.

**Keywords:** ANIT, Liver Function, Biochemical Markers, Hepatic

## Introduction

Cholestasis is a frequent liver disease that occurs as a result of impaired synthesis, secretion or flow of bile, causing the build-up of hepatotoxic bile acids in the liver cells and blood [1]. This condition is known to be associated with other diverse diseases like drug-induced liver injury (DILI) or intrahepatic cholestasis of pregnancy, primary biliary cholangitis (PBC) and primary sclerosing cholangitis (PSC). Untreated cholestasis can result in fibrosis, liver failure or hepatocellular carcinoma gradually [2]. Bile acids are produced from cholesterol via the classical pathway via CYP7A1 or the alternative pathway via CYP27A1 [3]. They are then stored in the gallbladder and secreted into the intestine to help in the digestion and absorption of lipids and the fat-soluble vitamins (A, D, E and K.). Among them, one is farnesoid X receptor (FXR), which has a pivotal role in control of bilirubin export by SHP and FGF15 and control essential transporters like BSEP and NTCP [4]. There is also the

membrane receptor of TGR5 which helps to increase the production of cAMP, bile flow and the regulation of enterohepatic circulation [5].

An experimental agent for induction of intra hepatic cholestasis in rodents is alpha-naphthylisothiocyanate ( ANIT ). ANIT is moved to bile canaliculus by means of conjugation with glutathione within hepatocytes after which it is broken down and directly damages the biliary epithelium [6]. This results in inflammatory conditions, cellular destruction, liver enzymes (ALT, AST, ALP, GGT) increase, and serum total bilirubin and bile acid increase. Another effect of ANIT is hepatotoxicity, which is linked to the dysregulation of major molecular pathways, such as the activation of the AMPKFXR axis, amplification of oxidative stress via TLR4LPS signaling, and Egr-1 induction to promote inflammatory reactions [7;8].

Despite the idea that ursodeoxycholic acid (UDCA), at the first line of treatment, is the most suitable drug with its cytoprotective and choleric effects, most patients with PBC cannot respond adequately to treatment, which is about 40 percent [9]. Furthermore, pharmacological FXR agonists such as obeticholic acid (OCA) remain limited by adverse effects and variable therapeutic efficacy [10]. These limitations point to an urgent need to understand at a molecular level the role of FXR, Nrf2, and AMPK in cholestasis development more thoroughly in the ANIT model for development of safer and more effective therapeutic interventions [11].

Accordingly, the purpose of this study is to assess the hepatotoxic effects of ANIT (100 mg/kg) in Wistar rats by measuring hepatic function markers (ALT, AST, ALP, GGT, TBIL, TBA) and investigating the histological changes associated and focusing on elucidating the possible molecular mechanisms concerned with bile acid regulation and oxidative stress.

## Materials and Methods

### 1. Animals and Living Conditions

This study involved use of ten male Wistar rats aged between 5 and 6 weeks and weighing 100-150g because it is a strain that has been identified as a good model in hepatotoxicity research [12]. The animals were housed in a controlled environment with temperature and humidity regulated at 24±2 °C and 12/12-hour light/dark cycle respectively. The standard chow and water were given to rats ad libitum and animals were observed every day in order to confirm their health status and to eliminate any form of stress in accordance with established animal care principles in biomedical research [13].

### 2. Chemicals and Equipment

Cholestasis was induced experimentally with the help of  $\alpha$ -naphthyl isothiocyanate (ANIT) (Sigma Aldrich; purity 95%) and corn oil was used as a solvent, which was stable and could be passed through the gastrointestinal tract by gavage [14]. Other reagents were 10 percent formalin to fix the tissues, gradient ethanol solution, and xylene to dehydrate and clear tissues, and phosphate-buffered saline (PBS) to wash the tissues before fixation [15].

The supplies used were micropipettes with different volumes to prepare reagents and doses, Eppendorf tubes to store samples, a centrifuge to separate serum, a 37 °C incubator to perform ELISA assays, and a microplate reader to run biochemical assays. Histological preparation was done on a tissue-processing unit, which consisted of a microtome that performed the cut and a light microscope that examined the sections.

### 3. Experimental Design

The rats were selected randomly under two groups of five rats each. The control group was given just the corn oil at a dose of 1 mL/kg as oral gavage to make sure that whatever may be the result of the alteration on biochemical parameters would be accredited to the tested compound and not to the vehicle. ANIT group was given a dose of 100 mg/kg ANIT in 1 mL of corn oil orally . The dose was transferred via an oral gavage tube, thus making the dose arrive in the gastrointestinal tract accurately. Animals were subsequently allowed to go over 48 hours, which is the experimentally determined duration taken by ANIT induced hepatotoxicity to evolve, before being sacrificed and sampled.

#### 4. Blood Collection and Serum Preparation

Rats were anesthetized with diethyl ether after 48 hours lest they be exposed to pain in the process of sampling. To get enough and quality samples, blood was taken through cardiac puncture. The blood was put in gel separator tubes and centrifuged at 3600 rpm and 20 minutes. Clear serum obtained was removed into sterile tubes and kept at -20C until biochemical analysis.

#### 5. Biochemical Evaluation of hepatic Performance.

Several biochemical tests were conducted with commercial test sets that had been validated and precise spectrophotometric methods:

##### 5.1 ALT and AST (IFCC Method)

The actions of ALT and AST were established upon the observance of the reduction in NADH absorbance at 340 nm.

In the ALT test, the alanine is transformed into pyruvate which is eventually reduced by LDH releasing the NADH to oxidize.

In AST assay, aspartate will be converted to oxaloacetate and subsequently reduced by MDH, which also uses the NADH.

The absorbance rate is proportional to the activity of the enzyme.

##### 5.2 ALP (DGKC Method)

The activity of ALP was quantified in terms of hydrolyzing of p- nitrophenyl phosphate to p-nitrophenol, which is a yellow colored compound that was measured at 405 nm. When the absorbance is higher it means that the enzyme is more active.

##### 5.3 GGT (ELISA)

The concentration of GGT was determined with the help of an ELISA kit. One hour incubation of samples at 37 °C was part of the pre-coating procedure of wells with a respective antibody. The color was measured using a colorometer at 450 nm after the biotinylated antibodies, an enzyme conjugate, and a chromogenic substrate. This is a measure of GGT in serum.

##### 5.4 Total Bilirubin (Diazotization Method)

The total bilirubin is reacted with diazotized sulfanilic acid to give a pink azobilirubin complex the absorbance of which is read at 540 nm. Bilirubin concentration(20) is correlated with the color intensity.

##### 5.5 Total Bile Acids (3 $\alpha$ -HSD Enzymatic Assay)

The 3-alpha-HSD converts bile acids to 3-ketosteroids with the decrease in Thio-NAD to Thio-NADH that possesses a distinct absorbance of 405 nm. The absorbance that is generated is dependent on the level of bile acid in the sample.

#### 6. Liver Histopathology

Following sacrifice, liver tissues were removed and washed thoroughly with PBS to get rid of the leftover blood. Tissues were fixed in 10% formalin over the course of 24 hours to maintain tissue structure. They were then dried using a graded ethanol series (70-100%), cleared in xylene and embedded in paraffin.

Paraffin blocks were cut in 5  $\mu$ m slices using a microtome, stained with a hematoxylin and eosin (H&E) stain and observed under a light microscope at 100 x and 400 x magnifications to assess inflammation, necrosis, ductal obstruction and other pathological conditions of ANIT-induced cholestasis.

## Results

### 1. Alanine Aminotransferase (ALT, U/L)

ALT is a direct biochemical measure of hepatocellular integrity and high values indicate hepatocyte damage.

In Table 1, ANIT evidently raises the ALT activity in all the treated rats, in comparison with the control group. The control rat values were between 25.70 and 28.32 U/L, but in the ANIT group the values were significantly high with ranges of 45.51-49.75 U/L[13].

**Table 1.** ALT Levels (U/L).

| Rat           | Control                       | ANIT                          |
|---------------|-------------------------------|-------------------------------|
| 1             | 28.322                        | 49.749                        |
| 2             | 27.547                        | 45.512                        |
| 3             | 25.705                        | 46.043                        |
| 4             | 25.998                        | 47.064                        |
| 5             | 26.422                        | 46.746                        |
| Mean $\pm$ SD | 26.80 $\pm$ 1.10 <sup>b</sup> | 47.02 $\pm$ 1.64 <sup>a</sup> |

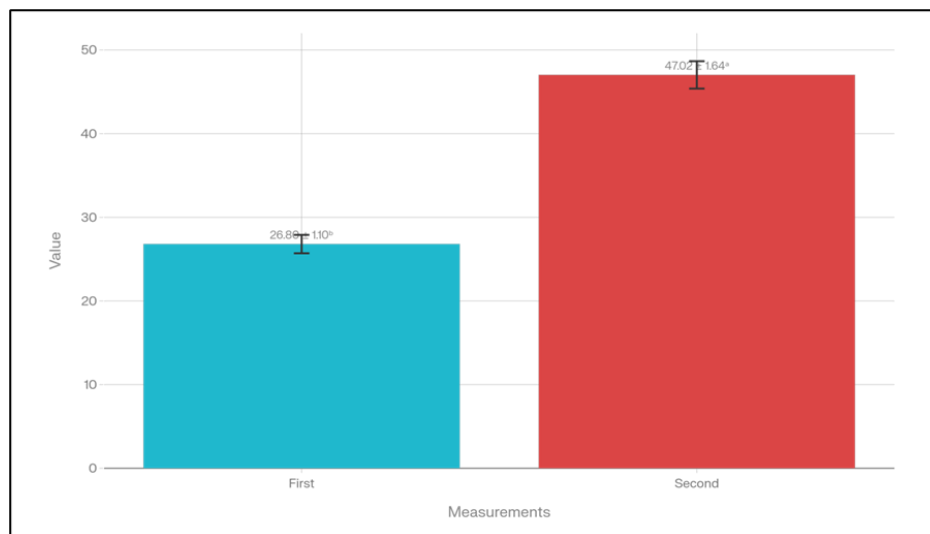


**Figure 1.** Rat Control ANIT group means with standard deviations.

The means of the ALT were 26.80 and 47.02, respectively, in the control and ANIT groups; in other words, the level changed by about 75 per cent[13]. Strong evidence of high hepatocellular injury caused by ANIT is strongly suggestive of the fact that ANIT is a well-established trigger of inflammation and focal hepatocyte necrosis.

## 2. Aspartate Aminotransferase (AST, U/L)

The results showed that after administration of ANIT, AST increased nearly in a two-fold manner with the mean value of the AST increasing to 55.07 U/L in the control animals as compared to ANIT-treated animals[11]. The values were also very high in all five rats indicating a homogeneous toxic response.

**Table 2.** AST Levels (U/L).

| Rat           | Control                       | ANIT                          |
|---------------|-------------------------------|-------------------------------|
| 1             | 25.979                        | 59.472                        |
| 2             | 29.359                        | 52.713                        |
| 3             | 24.730                        | 53.313                        |
| 4             | 27.157                        | 56.227                        |
| 5             | 30.576                        | 53.604                        |
| Mean $\pm$ SD | 27.56 $\pm$ 2.40 <sup>b</sup> | 55.07 $\pm$ 2.81 <sup>a</sup> |

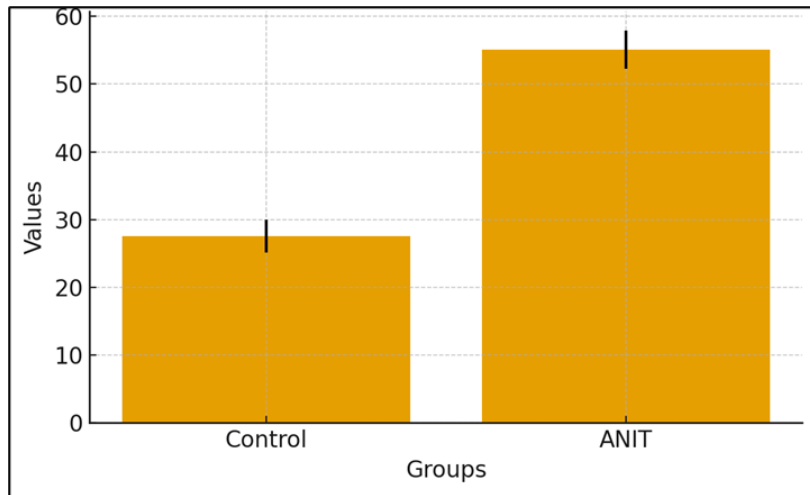


**Figure 2.** AST Levels in control and ANIT groups (mean ± SD).

The strong increase in AST indicates massive mitochondrial stress and general hepatocellular injury- both characteristic of ANIT-induced liver injury.

**3. Alkaline Phosphatase (ALP, U/L)**

The ALP also rose significantly, on a steady level, in the control group (100.68 U/L) to 353.45 in the ANIT-treated group-a 3- to 4-fold increase [13].

**Table 3.** ALP Levels (U/L).

| Rat       | Control                          | ANIT                              |
|-----------|----------------------------------|-----------------------------------|
| 1         | 102.942                          | 327.209                           |
| 2         | 101.521                          | 335.067                           |
| 3         | 98.867                           | 349.602                           |
| 4         | 98.245                           | 416.891                           |
| 5         | 101.833                          | 338.500                           |
| Mean ± SD | <b>100.68 ± 2.02<sup>b</sup></b> | <b>353.45 ± 36.37<sup>a</sup></b> |

This is a very high increase, which is highly suggestive of either biliary epithelial injury or cholestatic obstruction, which is exactly the pathophysiology of ANIT, which leads to the injury of bile ductulus epithelial cells.

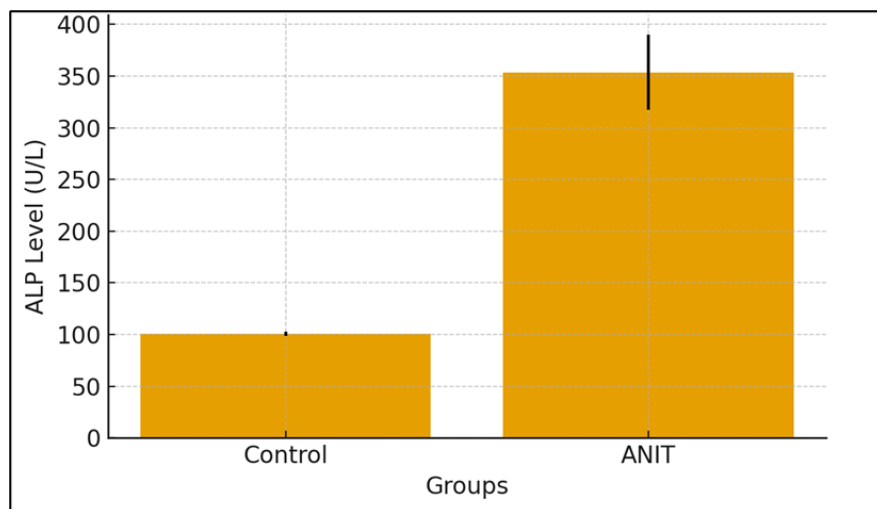


**Figure 3.** ALP Levels in control and ANIT groups (mean ± SD).

#### 4. Gamma-Glutamyl Transferase (GGT, U/L)

The level of GGT went up by over three times in the ANIT group (mean 730.63 U/L) compared with the control group (236.82 U/L). Several animals had very high values, more than 800 U/L[16].

**Table 4.** GGT Levels (U/L).

| Rat           | Control  | ANIT   |
|---------------|--|--|
| 1             | 226.651  | 706.906  |
| 2             | 223.137  | 654.779  |
| 3             | 229.651  | 718.426  |
| 4             | 257.651  | 817.138  |
| 5             | 246.999  | 755.891  |
| Mean $\pm$ SD | <b>236.82 <math>\pm</math> 14.83<sup>b</sup></b> | <b>730.63 <math>\pm</math> 60.39<sup>a</sup></b> |

This sharp elevation points to massive injury to cholangiocytes, one of the manifestations of ANIT-induced cholangiopathy.

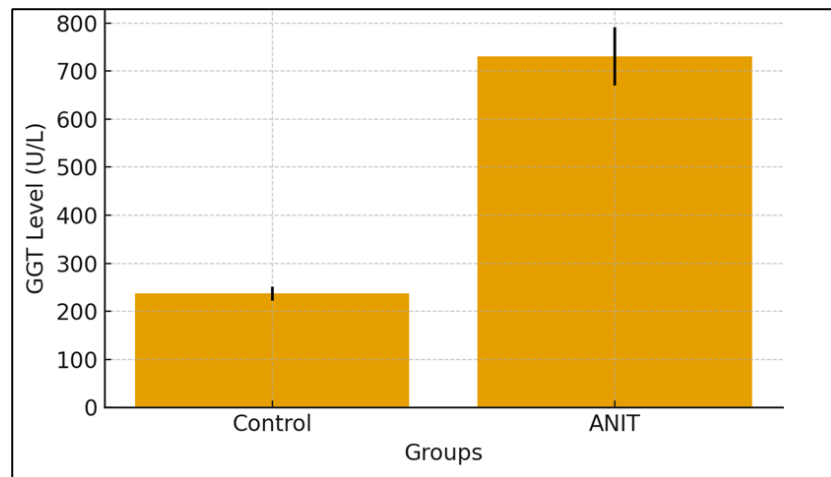


**Figure 4.** GGT Levels in control and ANIT groups (mean  $\pm$  SD).

#### 5. Total Serum Bilirubin (TSB) and Total Bile Acids (TBA)

Table 5 shows a substantial increase of both signs of cholestasis. TSB went from 1.06 mg/dL to 1.73 mg/dL, and it was showing that they were not clearing bilirubin well. The following are the significant changes in hepatic enzymes and liver function tests: - TBA increased significantly from 5.30 micro-mol / L to 16.36 micro-mol/L, almost a three-fold rise in levels based on severe disruption of the bile flow and gross accumulation of bile acids in circulation [17].

**Table 5.** TSB and TBA Levels.

| Rat           | TSB Control                                   | TSB ANIT                                      | TBA Control                                   | TBA ANIT                                       |
|---------------|---|---|---|--|
| 1             | 1.115   | 1.979   | 4.365   | 13.137   |
| 2             | 1.050   | 1.612   | 5.608   | 16.824   |
| 3             | 1.030   | 1.552   | 4.928   | 16.357   |
| 4             | 1.059   | 1.932   | 7.327   | 19.862   |
| 5             | 1.058   | 1.556   | 4.286   | 15.593   |
| Mean $\pm$ SD | <b>1.06 <math>\pm</math> 0.03<sup>b</sup></b> | <b>1.73 <math>\pm</math> 0.21<sup>a</sup></b> | <b>5.30 <math>\pm</math> 1.25<sup>b</sup></b> | <b>16.36 <math>\pm</math> 2.42<sup>a</sup></b> |

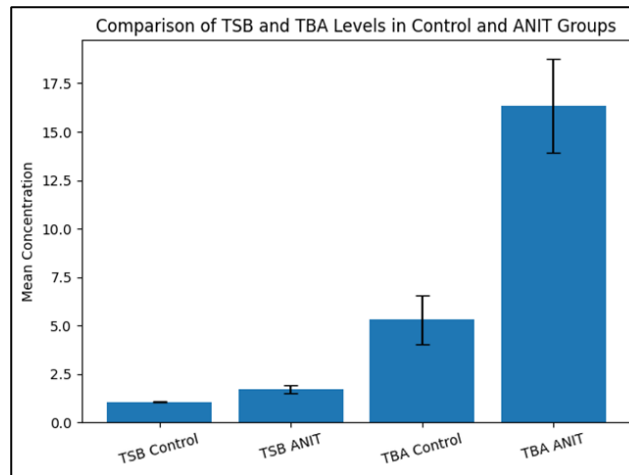


**Figure 5.** Comparison of TSB and TBA levels in control and ANIT groups.

The high levels of both parameters confirm the presence of severe cholestasis due to ANIT, in accordance with biochemical and histological signs of a biliary disorder.

#### 6. Reactive Oxygen Species (ROS) Levels at Various Levels of Hydrogen Peroxide (H<sub>2</sub>O<sub>2</sub>)

Table 6 shows a progressive increase in intracellular ROS with increasing concentrations of H<sub>2</sub>O<sub>2</sub>. ROS levels are minimal at 0 mM; they gradually increase at 0.5 mM and 5 mM, and attain significantly elevated levels at 10 mM and 25 mM and eventually reach maximal levels at 50 mM. This dose dependent effect confirms that with higher oxidative stimulus there is a direct escalation in ROS production [18]. These results clearly establish a concentration-dependent oxidative stress response.

**Table 6.** ROS Levels at Different H<sub>2</sub>O<sub>2</sub> Concentrations.

| H <sub>2</sub> O <sub>2</sub> (mM) | ROS Level (Absorbance Units) |
|------------------------------------|------------------------------|
| 0                                  | 0.15 ± 0.01                  |
| 0.5                                | 0.22 ± 0.02                  |
| 5                                  | 0.37 ± 0.03                  |
| 10                                 | 0.55 ± 0.04                  |
| 25                                 | 0.78 ± 0.05                  |
| 50                                 | 1.12 ± 0.06                  |

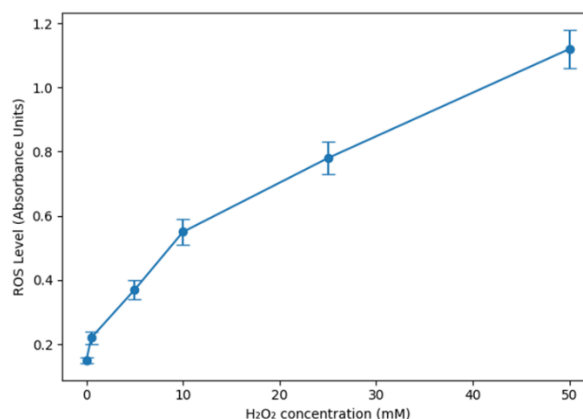


**Figure 6.** Effect of H<sub>2</sub>O<sub>2</sub> concentration on ROS generation.

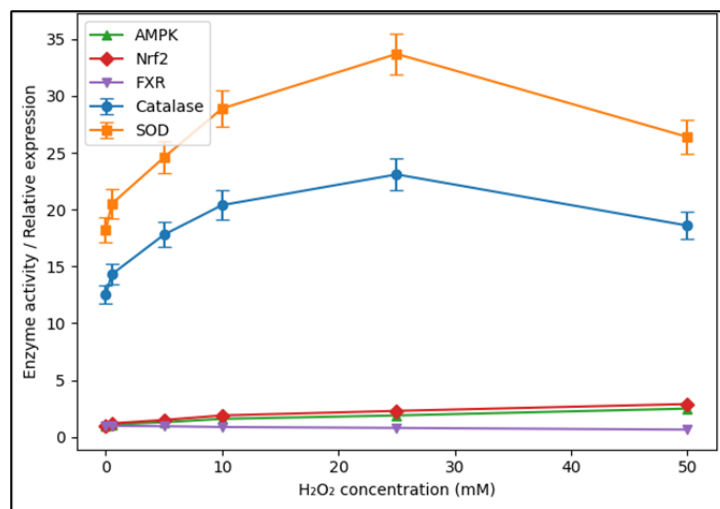
#### 7. Antioxidant Enzymes Activity and Molecular Pathway Modulation

Table 7 demonstrates the increased catalase and SOD activity over time that occur with increasing concentrations of H<sub>2</sub>O<sub>2</sub> from baseline to intermediate concentrations and represent a

compensatory antioxidant response. However, both these enzymes show low activity at 50 mM, which is suggestive of antioxidant system exhaustion at extreme oxidative stress [19]. AMPK and Nrf2 concentrations rise uniformly between all concentrations which indicates activation of energy-sensing and cytoprotective systems in response to oxidative stress [20]. In comparison, FXR concentrations show a slow decrease in response to the inhibition of the homeostasis of bile-acids pathways during oxidative insult.

**Table 7.** Antioxidant Enzymes and Signal cascades during Oxidative Stress.

| H <sub>2</sub> O <sub>2</sub> (mM) | Catalase (U/mg) | SOD (U/mg) | AMPK | Nrf2 | FXR  |
|------------------------------------|-----------------|------------|------|------|------|
| 0                                  | 12.5 ± 0.8      | 18.2 ± 1.1 | 1.0  | 1.0  | 1.0  |
| 0.5                                | 14.3 ± 0.9      | 20.5 ± 1.3 | 1.1  | 1.2  | 0.98 |
| 5                                  | 17.8 ± 1.1      | 24.6 ± 1.4 | 1.3  | 1.5  | 0.95 |
| 10                                 | 20.4 ± 1.3      | 28.9 ± 1.6 | 1.6  | 1.9  | 0.88 |
| 25                                 | 23.1 ± 1.4      | 33.7 ± 1.8 | 1.9  | 2.3  | 0.80 |
| 50                                 | 18.6 ± 1.2      | 26.4 ± 1.5 | 2.5  | 2.9  | 0.65 |



**Figure 7.** Effect of H<sub>2</sub>O<sub>2</sub> on Antioxidant enzymes and signaling pathways.

Collectively, these patterns indicate that an increase in oxidative stress activates the phosphoprotein protein kinase A (AMPK) and Nrf2, boosts the activity of antioxidant enzymes up to some threshold, and inhibits FXR, which disrupts the mechanism regulating the regulation of bile acid.

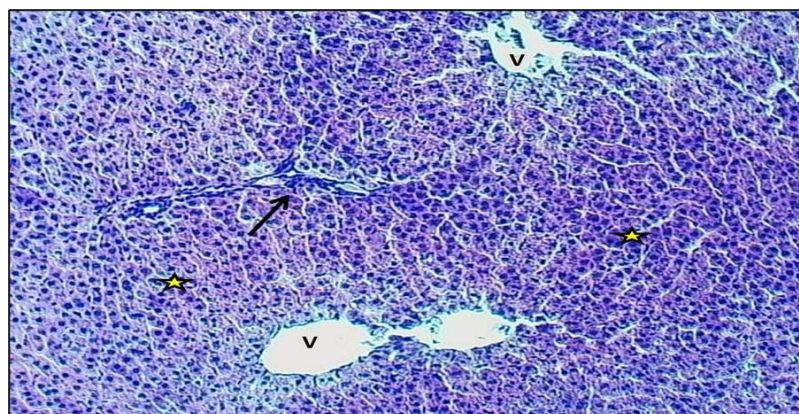


**Figure 8.** Section of hepatic lobule (Control group-A) shows: Normal appearance- portal triad (Arrow), normal central vein ( V) with normal arrangement of hepatic cords (Asterisk). H&E stain. 100x.

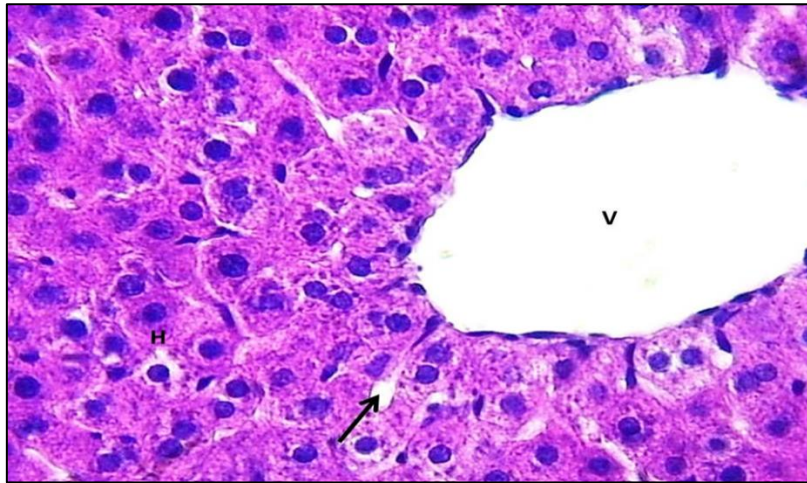


**Figure 9.** Which shows a section of a hepatic lobule from the control group (A), you can see a normal-looking central vein (V). The surrounding hepatocytes (H) and sinusoids (indicated by the arrow) also appear healthy and typical. This image was stained with H&E and viewed at 400x magnification.

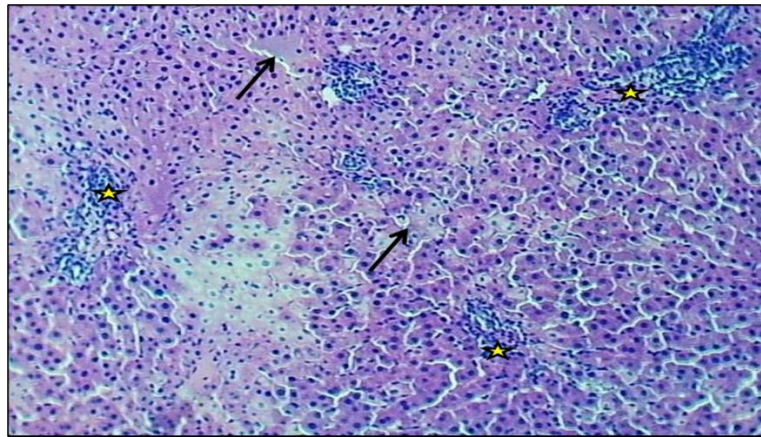


**Figure 10.** Cross-section of a hepatic lobule from Group B (induction group) reveals widespread areas of liver cell death, with lots of white blood cells gathered around (marked with asterisks). The normal structure of the liver cords is broken up quite a bit, and the hepatocytes look heavily hyalinized (indicated by arrows). Stained with H&E, magnification 100x.

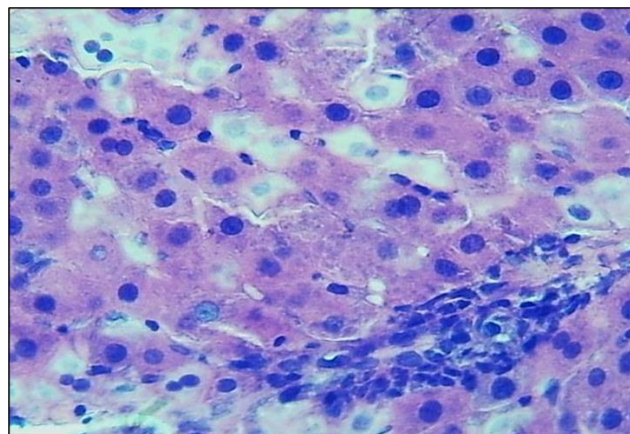


**Figure 11.** Shows a cross-section of a hepatic lobule from Group B after induction. It reveals several areas of severe liver cell death, with many white blood cells gathered around. The hepatocytes also look heavily hyalinized, indicating significant damage. The image was stained with H&E and viewed at 400x magnification.

## Discussion

The overall results of this study paint a clear picture of how ANIT causes damage to the liver and bile system. We see significant changes in liver enzymes, markers related to cholestasis, levels of oxidative stress, and the body's molecular responses. Notably, the levels of ALT and AST enzymes were greatly increased in mice treated with ANIT, as shown in Tables 1 and 2. This clearly indicates that there is serious damage happening to the liver cells. ALT, which is more specific to liver cells, increased by about 75%, while AST almost doubled. That suggests there's not just damage to the cell membranes but maybe some injury to the mitochondria too, since AST is plentiful in mitochondria. This pattern fits with the typical signs of liver toxicity seen with ANIT [21;22]. Basically, when the body processes ANIT, it creates reactive compounds that cause inflammation and small areas of cell death in the liver [23].

This is further supported by the dramatic elevation of the ALP and GGT levels (Tables 3 and 4) which point out the cholestatic character of ANIT toxicity. Both of them are classical indicators of biliary epithelial injury and their three to fourfold elevation signals the blockage or inflammation of the intrahepatic bile ducts [24]. ANIT selectively accumulates in cholangiocytes where it is glutathione-dependent conjugated and secreted by the biliary system resulting in epithelial disruption and impaired activity of the transporters [25]. The very high GGT results, > 800 U/L in some animals, indicate severe cholangiocellular stress, as would be seen with ductular reaction and biliary proliferation in experimental models of cholestasis [26].

These biochemical derangements are reflected in the very high values of TSB and TBA (Table 5). The elevation of bilirubin indicates dysfunction of hepatic excretory function, whereas the three-fold elevation of total bile acids indicates gross dysfunction of bile acid transport systems [27]. Due to their detergent-like properties, bile acids, when accumulated inside cells, favour mitochondrial damage, inflammation and oxidative stress [28]. Basically, these effects are pretty much tied to lower FXR activity because FXR controls how bile acids stay balanced in the body. It does this by regulating things like BSEP, NTCP, SHP, and other transporters [29]. Thus, the suppression of FXR expression as found in Table 7 is probably a contributing factor toward uncontrolled accumulation of bile acids and further enhances hepatobiliary injury [30].

The data on Oxidative stress data (Table 6) also adds another mechanistic dimension. As they increased the H<sub>2</sub>O<sub>2</sub> treatment, the amount of ROS released by the liver cells went up in a straight line. This shows that the cells become more vulnerable to oxidative damage as the dose of H<sub>2</sub>O<sub>2</sub> increases. The pattern of antioxidant enzyme activity for Table 7 is consistent with this mechanism in that the activities of catalase and SOD increased at low and moderate concentrations of H<sub>2</sub>O<sub>2</sub> but decreased at 50 mM; reflecting exhaustion of cellular antioxidant defenses [31]. Excess of ROS may lead to disrupted mitochondrial respiratory function, lipid peroxidation and elevated hepatocellular damage, especially against cholestasis [32].

The molecular pathway results offer a compelling framework for making sense out of these events. The regular elevation of AMPK is suggestive of energetic stress caused by disrupted mitochondrial function induced by ANIT and ROS accumulation [33]. AMPK activation is a classic response to depletion of ATP and is to restore metabolic equilibrium. Concurrently, Nrf2 upregulating represents a compensatory antioxidant response intended to turn on detoxifying and cytoprotective genes [34]. However, despite a significant activation of Nrf2, the inability to control ROS at the highest oxidative load shows that the amount of damage is higher than the antioxidant system can control [35].

The way FXR, AMPK, and Nrf2 work together seems to form a really tight and connected system of regulation. Decreased FXR Activity Increased cholestatic bile acid retention Increased ROS Levels Activation of AMPK and Nrf2 Increased oxidative stress results in excessive stimulation of antioxidant enzymes and suppression of hepatocellular resilience [36]. Together, these mechanisms give a clear, step-by-step explanation for the biochemical and tissue changes we've seen.

Overall, looking at all seven tables together, it's clear that ANIT causes both liver cell and bile duct damage. This damage seems to come from too much oxidative stress, problems with getting rid of bile acids, and changes in how certain molecules signal inside the cells. The mix of shutting down

FXR while activating AMPK and Nrf2 shows how the cells are really fighting to cope with the increasing bile acid buildup and the redox imbalance [37, 38]. These findings show that oxidative stress and problems with bile acid regulation are key factors behind the liver and bile duct damage caused by ANIT.

## Conclusion

This study shows that giving ANIT at 100 mg/kg creates a reliable model of intrahepatic cholestasis in Wistar rats. The rats develop clear signs of liver trouble, with big jumps in liver enzymes. The high levels of ALT and AST indicate serious liver cell damage, while the spikes in ALP and GGT point to injury in the bile ducts and problems with bile flow. At the same time, total bilirubin levels go up, showing that bile processing is really affected. Looking at the tissue under the microscope confirms what the biochemistry suggested. There's clear damage: multiple spots of liver cell death, infiltration of inflammatory cells, and disruption of the normal structure of the liver cords. These are typical signs of liver toxicity caused by ANIT. When we checked oxidative stress, we saw that as the dose increased, so did the levels of reactive oxygen species (ROS). The body tried to fight back by activating antioxidant enzymes, but it wasn't enough to fully counteract the damage. On a molecular level, the response seems to be coordinated but still out of balance, indicating a complex yet disrupted regulatory process.

Overall, these findings show that ANIT causes a complicated type of liver and bile duct damage. This damage seems to come from a buildup of bile acids, increased oxidative stress, and disruptions in important cell signaling pathways. The study highlights how useful the ANIT model is for exploring the underlying molecular causes of cholestasis. It also sets the stage for future research looking into treatments that target FXR, Nrf2, and AMPK pathways.

## REFERENCES

- [1] G. M. Hirschfield and E. J. Heathcote, "Cholestasis and cholestatic syndromes," *Curr. Opin. Gastroenterol.*, vol. 25, no. 3, pp. 175–179, 2009, doi: 10.1097/MOG.0b013e32832914b4.
- [2] C. D. Fuchs *et al.*, "Bile acid metabolism and signalling in liver disease," *J. Hepatol.*, vol. 82, no. 1, pp. 134–153, 2025, doi: 10.1016/j.jhep.2024.09.032.
- [3] T. M. Šarenac and M. Mikov, "Bile acid synthesis: From nature to the chemical modification and synthesis and their applications as drugs and nutrients," *Front. Pharmacol.*, vol. 9, p. 939, 2018, doi: 10.3389/fphar.2018.00939.
- [4] J. Y. Chiang, "Bile acid metabolism and signaling," *Compr. Physiol.*, vol. 7, no. 3, pp. 923–952, 2017, doi: 10.1002/j.2040-4603.2013.tb00517.x.
- [5] T. W. Pols *et al.*, "The bile acid membrane receptor TGR5 as an emerging target in metabolism and inflammation," *J. Hepatol.*, vol. 54, no. 6, pp. 1263–1272, 2011, doi: 10.1016/j.jhep.2010.12.004.
- [6] L. Yu *et al.*, "SRT1720 alleviates ANIT-induced cholestasis in a mouse model," *Front. Pharmacol.*, vol. 8, p. 256, 2017, doi: 10.3389/fphar.2017.00256.
- [7] T. Yang *et al.*, "Early indications of ANIT-induced cholestatic liver injury: Alteration of hepatocyte polarization and bile acid homeostasis," *Food Chem. Toxicol.*, vol. 110, pp. 1–12, 2017, doi: 10.1016/j.fct.2017.09.051.
- [8] S. Thakur *et al.*, "Biomarkers of hepatic toxicity: An overview," *Curr. Ther. Res.*, vol. 100, p. 100737, 2024, doi: 10.1016/j.curtheres.2024.100737.
- [9] F. Nevens *et al.*, "A placebo-controlled trial of obeticholic acid in primary biliary cholangitis," *N. Engl. J. Med.*, vol. 375, no. 7, pp. 631–643, 2016.
- [10] M. Li, S. Y. Cai, and J. L. Boyer, "Mechanisms of bile acid mediated inflammation in the liver," *Mol. Aspects Med.*, vol. 56, pp. 45–53, 2017, doi: 10.1016/j.mam.2017.06.001.
- [11] C. Audousset, T. McGovern, and J. G. Martin, "Role of Nrf2 in disease: Novel molecular mechanisms and therapeutic approaches—pulmonary disease/asthma," *Front. Physiol.*, vol. 12, p. 727806, 2021, doi: 10.3389/fphys.2021.727806.
- [12] M. Bhat *et al.*, "The basis of liver regeneration: A systems biology approach," *Ann. Hepatol.*, vol. 18, no. 3, pp. 422–428, 2019, doi: 10.1016/j.aohp.2018.07.003.

- [13] National Research Council, *Guide for the Care and Use of Laboratory Animals*, 8th ed. Washington, DC, USA: National Academies Press, 2011.
- [14] L. Chen *et al.*, "Mechanism of paeoniflorin on ANIT-induced cholestatic liver injury using integrated metabolomics and network pharmacology," *Front. Pharmacol.*, vol. 12, p. 737630, 2021, doi: 10.3389/fphar.2021.737630.
- [15] J. D. Bancroft and M. Gamble, *Theory and Practice of Histological Techniques*, 8th ed. Amsterdam, Netherlands: Elsevier, 2019.
- [16] J. H. Suh *et al.*, "Bile acid regulation of xenobiotic nuclear receptors on the expressions of orosomucoids in the liver," *Am. J. Physiol. Endocrinol. Metab.*, vol. 328, no. 6, pp. E940–E951, 2025, doi: 10.1152/ajpendo.00417.2024.
- [17] E. Gijbels *et al.*, "Rodent models of cholestatic liver disease: A practical guide for translational research," *Liver Int.*, vol. 41, no. 4, pp. 656–682, 2021, doi: 10.1111/liv.14800.
- [18] S. Parasuraman, R. Raveendran, and R. Kesavan, "Blood sample collection in small laboratory animals," *J. Pharmacol. Pharmacother.*, vol. 1, no. 2, pp. 87–93, 2010, doi: 10.4103/0976-500X.72350.
- [19] R. Zhu, Y. Wang, L. Zhang, and Q. Guo, "Oxidative stress and liver disease," *Hepatol. Res.*, vol. 42, no. 8, pp. 741–749, 2012, doi: 10.1111/j.1872-034X.2012.00996.x.
- [20] Q. Ma, "Role of Nrf2 in oxidative stress and toxicity," *Annu. Rev. Pharmacol. Toxicol.*, vol. 53, pp. 401–426, 2013, doi: 10.1146/annurev-pharmtox-011112-140320.
- [21] A. A. Santos *et al.*, "Primary bile acid shapes peripheral immunity in inflammatory bowel disease-associated primary sclerosing cholangitis," *Clin. Sci.*, vol. 139, no. 12, pp. 703–716, 2025, doi: 10.1042/CS20256078.
- [22] A. Mansouri, C. H. Gattolliat, and T. Asselah, "Mitochondrial dysfunction and signaling in chronic liver diseases," *Gastroenterology*, vol. 155, no. 3, pp. 629–647, 2018, doi: 10.1053/j.gastro.2018.06.083.
- [23] M. Belka *et al.*, "Activation of Nrf2 and FXR via natural compounds in liver inflammatory disease," *Int. J. Mol. Sci.*, vol. 25, no. 20, p. 11213, 2024, doi: 10.3390/ijms252011213.
- [24] M. Constantinides *et al.*, "A genes and health recall study of intrahepatic cholestasis of pregnancy and cholestatic liver disease," *Commun. Med.*, vol. 5, p. 531, 2025, doi: 10.1038/s43856-025-01228-4.
- [25] Y. Tanaka *et al.*, "ANIT-induced intrahepatic cholestasis alters hepatobiliary transporter expression via Nrf2-dependent and independent signaling," *Toxicol. Sci.*, vol. 108, no. 2, pp. 247–257, 2009, doi: 10.1093/toxsci/kfp020.
- [26] M. Xing *et al.*, "Characteristics of peripheral blood gamma-glutamyl transferase in different liver diseases," *Medicine*, vol. 101, no. 1, p. e28443, 2022, doi: 10.1097/MD.00000000000028443.
- [27] M. Asensio *et al.*, "Etiopathogenesis and pathophysiology of cholestasis," *Explor. Dig. Dis.*, vol. 1, no. 2, pp. 97–117, 2022, doi: 10.37349/edd.2022.00008.
- [28] R. H. Ali *et al.*, "The relevance of mitochondrial DNA mutation in human diseases and forensic sciences," *Al-Nahrain J. Sci.*, vol. 28, no. 1, pp. 96–106, 2025, doi: 10.22401/ANJS.28.1.11.
- [29] M. Stofan and G. L. Guo, "Bile acids and FXR: Novel targets for liver diseases," *Front. Med.*, vol. 7, p. 544, 2020, doi: 10.3389/fmed.2020.00544.
- [30] G. Song *et al.*, "Bile acids affect intestinal barrier function through FXR and TGR5," *Front. Med.*, vol. 12, p. 1607899, 2025, doi: 10.3389/fmed.2025.1607899.
- [31] V. Keitel, C. Dröge, and D. Häussinger, "Targeting FXR in cholestasis," in *Bile Acids and Their Receptors*, S. Fiorucci and E. Distrutti, Eds. Cham, Switzerland: Springer, 2019, vol. 256, doi: 10.1007/164\_2019\_231.
- [32] M. Valko *et al.*, "Free radicals and antioxidants in normal physiological functions and human disease," *Int. J. Biochem. Cell Biol.*, vol. 39, no. 1, pp. 44–84, 2007, doi: 10.1016/j.biocel.2006.07.001.
- [33] A. Allameh *et al.*, "Oxidative stress in liver pathophysiology and disease," *Antioxidants*, vol. 12, no. 9, p. 1653, 2023, doi: 10.3390/antiox12091653.
- [34] G. R. Steinberg and D. G. Hardie, "New insights into activation and function of the AMPK," *Nat. Rev. Mol. Cell Biol.*, vol. 24, no. 4, pp. 255–272, 2023, doi: 10.1038/s41580-022-00547-x.

- [35] V. Ngo and M. L. Duennwald, "Nrf2 and oxidative stress: A general overview of mechanisms and implications in human disease," *Antioxidants*, vol. 11, no. 12, p. 2345, 2022, doi: 10.3390/antiox11122345.
- [36] E. Petsouki, S. N. S. Cabrera, and E. H. Heiss, "AMPK and NRF2: Interactive players in the same team for cellular homeostasis?" *Free Radic. Biol. Med.*, vol. 190, pp. 75–93, 2022, doi: 10.1016/j.freeradbiomed.2022.07.014.
- [37] T. Li, M. N. Hasan, and L. Gu, "Bile acids regulation of cellular stress responses in liver physiology and diseases," *eGastroenterology*, vol. 2, no. 2, 2024, doi: 10.1136/egastro-2024-100074.
- [38] E. Hughes *et al.*, "Role of nuclear receptors, lipid metabolism, and mitochondrial function in the pathogenesis of diabetic kidney disease," *Am. J. Physiol. Renal Physiol.*, vol. 329, no. 4, pp. F510–F547, 2025, doi: 10.1152/ajprenal.00110.2025.